Abstract Volume
11th Swiss Geoscience Meeting

Lausanne, 15th – 16th November 2013

11. Geophysics and Rockphysics

sc | nat

Swiss Academy of Sciences
Akademie der Naturwissenschaften
Accademia di scienze naturali
Académie des sciences naturelles

UNIL | Université de Lausanne
Faculté des géosciences
et de l'environnement

11. Geophysics and Rockphysics

Marcel Frehner, Klaus Holliger

Swiss Geophysical Commission

TALKS:

11.1 Bakker R.R., Benson P.M.: Tensile fracturing and dyking in volcano-tectonic settings, a laboratory approach

11.2 Dafflon B., Hubbard S.S., Ulrich C., Peterson J.E., Wainwright H., Wu Y.: Investigating arctic permafrost behaviors using geophysical, point-scale and remote sensing data

11.3 Favero V., Ferrari A., Laloui L.: Shales retention properties and permeability through laboratory testing

11.4 Hunfeld U., Brenner O., Orlowsky D.: High-resolution CMP-refraction seismics in combination with refraction tomography, reflection seismics and surface wave analysis

11.5 Jougnot D., Rubino J.G., Rosas Carbajal M., Linde N., Holliger K.: Seismoelectric effects due to mesoscopic heterogeneities: numerical study for a fractured rock

11.6 Lupi, M., Saenger, E.H., Fuchs, F., Miller, S.A.: Focusing of seismic energy at LUSI mud volcano, Indonesia

11.7 Thüring M., Sayah S.M.: Assessment of the complex rock mass conditions for tunnels and underground caverns of the Hydropower Project Cerro del Águila (Peru)

11.8 Vouillamoz N., Abednego M., Deichmann N., Wust- Bloch H.G., Mosar J.: Lowering microseismic detection threshold by sonogram analysis for Fribourg area (Switzerland)

POSTERS:

P 11.1 Correia Demand J., Marillier F., Kremer K., Girardclos S.: Large mass wasting deposits in Lake Geneva off the city of Lausanne revealed by detailed reflection seismic data

P 11.2 Demirel S., Roubinet D., Irving J.: Modeling electric current flow in 3D fractured media

P 11.3 Koepke C., Irving J., Roubinet D.: Exploring the issue of model error in stochastic solutions to hydrogeophysical inverse problems

P 11.4 Kuhn P., Abdelfettah Y., Mauri G., Schill E., Vuataz F.: Improvement of the regional 3D modeling of deep geological structures with gravity: A case study in the Neuchatel Jura Mountains

P 11.5 Mo Y.K., Greenhalgh S.A., Karaman H., Robertsson J.: Laboratory seismic scale model study of reflection imaging beneath a distorting near surface zone

P 11.6 Peters, M., Poulet, T., Karrech, A., Regenauer- Lieb, K., Herwegh, M.: Material softening as a potential cause for the development of boudinage - an elasto-visco-plastic numerical modeling approach

P 11.7 Rosas Carbajal M., Linde N., Kalscheuer T., Vrugt J.: Two-dimensional probabilistic inversion of plane-wave electromagnetic data

P 11.8 Roubinet D., Irving J.: Discrete dual porosity modeling of electrical current flow in fractured media

P 11.9 Rubino J.G., Müller T.M., Guarracino L., Holliger K.: Seismic energy dissipation in fractured rocks

P 11.10 Shih P.J.R., Frehner M.: Numerical modeling and laboratory measurements of seismic properties in fractured fluid reservoirs

P 11.11 Subramaniyan S., Madonna C., Tisato N., Saenger E.H., Quintal B.: Seismic attenuation: Laboratory measurements in fluid saturated rocks

P 11.12 Tisato N., Quintal B., Podladchikov Y.: How much seismic energy is “stolen” by bubbles?

P 11.13 Wei Wu: Some new observations on dynamically induced fault slip

P 11.14 Zhang Y., Song S., Dalguer L., Clinton J.: Effect of network density and geometric distribution on non-linear kinematic source inversion models

11.1

Tensile fracturing and dyking in volcano-tectonic settings, a laboratory approach.

Bakker Richard R.[1], Benson Philip M.[2]

[1]*ETH Zürich, Department Erdwissenschaften, Structural Geology and Tectonics, Rock Deformation Laboratory. NO E 17, Sonneggstrasse 5, CH-8092*
[2] *Univerisity of Portsmouth, School of Earth and Environment. Burnaby Building, Burnaby Road, UK-PO1 3QL*

It is well known that magma ascends trough the crust by the process of dyking. During dyke movement crustal rocks, specifically the volcano's basement rocks, fracture due to the stress imposed by the ascending magma, thus providing conduits for magma transport. Dykes are frequently seen in the field and have been reproduced via numerical and analogue studies. However, a number of assumptions regarding rock mechanical behaviour frequently has to be made as such data are very hard to directly measure at the pressure/temperature conditions of interest: high temperatures at relatively shallow depths. Such data are key to simulating the magma intrusion dynamics through the lithologies that underlie the volcanic edifice.

Studies on the mechanical properties in a compressive regime have been successful. Volcanic rocks and basement rocks have been deformed at temperatures up to 1000 ˚C at relatively shallow pressures. However in the tensile regime, it remains a significant technical challenge to precisely reproduce the conditions of dyking in the lab. As a starting point, we are now testing an analogue material to replace the magma to avoid such high temperatures, relying of maintaining similar temperature/viscosity ratios between magma/country rock in the laboratory and the field. We chose PMMA (commonly known as plexiglass) for this task as it displays a large range in viscosities (log(visc)range = 10 –1) with temperatures between 100 and 300 ˚C, making it an excellent analogue material. In addition PMMA solidifies after the sample cools to permit post-test analysis of the pseudo dyke.

We have modified a traditional compression test / tri-axial test assembly setup to be able to use a Paterson High Pressure, High Temperature deformation apparatus. Sample setup consists of cylindrical rock samples with a 22mm diameter and a 8mm bore at their centre, filled with a PMMA cylinder. The top and lower parts of the rock sample are fitted with plugs, sealing in the PMMA. The assembly is then placed between ceramic pistons to ensure there are no thermal gradients across the sample. The assembly is jacketed to ensure the confining medium (Ar) cannot enter the assembly. When the assembly is brought to the desired PT conditions, a piston is driven up which pressurizes the conduit and the filler material. The filler material is "squeezed out" and thus transfers little to no stress on to the sample.

With the inner PMMA conduit pressurized, a sufficient pressure gradient between the inner and outer surfaces eventually cause the sample to deform and fail in the tensile regime. Tensile fractures can occur when the hoop stress exerted on the outer shell exceeds its tensile strength. The PMMA is then likely to flow into the newly formed fracture, depending on its viscosity and the fracture dimensions, allowing comparisons to be made between the temperature and intrusions dynamics of the simulated dyke process.

Ultimately this method will be extended to higher temperatures using NIST standard glasses and collected volcanic glasses for comparison to the analogue setup.

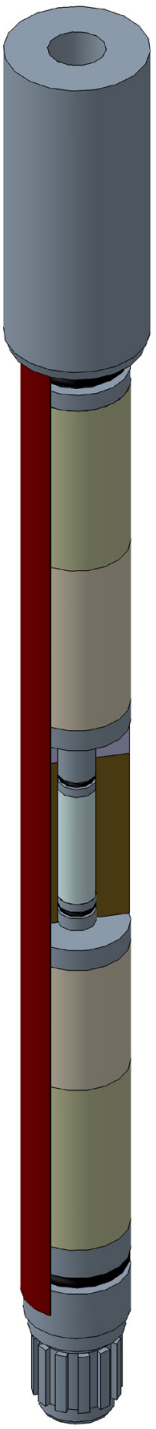

Figure 1, Schematic setup of the assembly

11.2

Investigating Arctic Permafrost Behaviors Using Geophysical, Point-Scale and Remote Sensing Data

Baptiste Dafflon[1], Susan S. Hubbard[1], Craig Ulrich[1], John E. Peterson[1], Haruko Wainwright[1] & Yuxin Wu[1]

[1]*Lawrence Berkeley National Laboratory (LBNL), Berkeley (CA), USA, (bdafflon@lbl.gov)*

The trajectory of arctic tundra ecosystem feedbacks to climate is recognized as a significant source of uncertainty in climate projections (e.g., Friedlingstein et al., 2006, Chapin et al., 2000). The uncertainty is associated with our inability to predict the behavior of components of the system as well as their interactions, including ecosystem energy balance, vegetation dynamics, and microbial soil organic carbon degradation associated with permafrost thaw, which could lead to significant CO_2 and CH_4 production (e.g., Schuur et al., 2009, Zimov et al., 2006). Improving understanding of arctic ecosystem functioning and parameterizing process-rich models that simulate feedbacks to a changing climate require advances in estimating the spatial and temporal variations in active layer, ice-wedge and permafrost soil properties.

As part of the DOE Next-Generation Ecosystem Experiments (NGEE-Arctic), we are developing advanced geophysical strategies to improve arctic subsurface imaging, and using the data to quantify land and subsurface co-variability and dynamics (e.g., Hubbard et al., 2013). Some specific objectives involve (i) developing advanced geophysical approaches for characterizing subsurface compartments and associated properties, including active layer, ice-wedges, ground-ice, saline layers, and permafrost with variable ice-content, (ii) quantifying relations between geomorphology, soil hydrological and geochemical properties, and geophysical properties, and (iii) integration of multi-scale and -resolution remote sensing, surface geophysical and point measurements to estimate properties (e.g., thaw depth, soil moisture, ice content and geochemical properties) and their uncertainty over scales that are relevant for modeling.

These objectives are pursued through various numerical developments, laboratory experiments, and field investigations. Field investigations have been performed at the NGEE site located in the Barrow Environmental Observatory (BEO) near the coastal village of Barrow (AK). This site shows a significant range of hydrological and geomorphological conditions; including low- to high- centered polygons and drained thaw lake basins (e.g., Sellmann et al., 1975). The data involved in this study includes point- scale (TDR, core analysis), surface-based geophysical (galvanic-coupled electrical resistance tomography (ERT), capacitively-coupled resistivity (CCR), electromagnetic induction (EMI), and Ground Penetrating Radar (GPR)), and remote sensing (LiDAR, Kite-based low-altitude aerial imaging) datasets.

In this presentation, we will describe several recent advances, including: (i) a novel parameter-estimation approach adapted to explore the solution non-uniqueness inherent to EMI and CCR data, which facilitates estimation of electrical conductivity variations in the active layer as well as trends in permafrost distribution over large areas (Dafflon et al., in press) (ii) high-resolution imaging of ice-wedges, permafrost and active layer using multi 2D electrical resistance tomography (ERT) at a high-spatial resolution, which enables identification of properties that vary substantially over length scales of less than a meter, (iii) understanding the complex resistivity electrical signature of arctic soils during freeze-thaw transitions at the laboratory and field scale, (iv) quantification of land-surface properties (using remote sensing data) and their co-variability with the subsurface properties.

Overall, the above advances enable improvements in estimating the i) thaw layer electrical conductivity distribution, which informs on soil water content distribution that strongly influences microbial activity, ii) soil ice-content distribution showing a variability from below one meter length scales to large trends over more than a kilometer, which is crucial to assess spatial variations in arctic permafrost dynamics, iii) distribution of low freezing-point saline layers that implies different comportment to temperature variations than surrounding permafrost, and iv) permafrost characteristics that correspond with changes in hydrogeomorphological surface expressions which is important to guide permafrost behavior zonation at larger spatial scale. Together, these advances are critical to guide investigations of carbon cycling processes and for improving the understanding of Arctic terrestrial environment characteristics and dynamics, in high resolution and over modeling-relevant spatial extents.

REFERENCES

Brown, J., 1969, Ionic Concenration Gradients in Permafrost Barrow, Alaska: Hanover, New Hampshire, Cold Regions Research and Engineering Laboratory, Corps of Engineers, US Army.

Chapin, F.S., McGuire, A.D., Randerson, J., Pielke, R., Baldocchi, D., et al., 2000, Arctic and boreal ecosystems of western North America as components of the climate system, Global Change Biology, 6, 211-223.

Dafflon B., Hubbard S.S., Ulrich, C., and Peterson J.E., Electrical conductivity imaging of active layer and permafrost in Arctic ecosystem, through advanced inversion of electromagnetic induction data, Vadose Zone Journal, in press,

doi:10.2136/vzj2012.0161.
Friedlingstein, P., Cox, P., Betts, R., Bopp, L., Von Bloh, W., et al., 2006, Climate-carbon cycle feedback analysis: Results from the C(4)MIP model intercomparison, Journal of Climate, 19(14), 3337-3353.
Hubbard, S.S., Gangodagamage, C., Dafflon, B., Wainwright, H., Peterson, J., et al., 2013, Quantifying and relating land-surface and subsurface variability in permafrost environments using LiDAR and surface geophysical datasets, Hydrogeology Journal, 21(1), 149-169.
Schuur, E.A.G., Vogel, J.G., Crummer, K.G., Lee, H., Sickman, J.O., et al., 2009, The effect of permafrost thaw on old carbon release and net carbon exchange from tundra, Nature, 459(7246), 556-559.
Sellmann, P.V., Brown, J., Lewellen, R.I., McKim, H., and Merry, C., 1975, The Classification And Geomorphic Implication of Thaw Lakes on the Arctic Coastal Plain, Alaska, US Army CRREL, Volume Research Report 344.
Zimov, S.A., Davydov, S.P., Zimova, G.M., Davydova, A.I., Schuur, E.A.G., et al., 2006, Permafrost carbon: Stock and decomposability of a globally significant carbon pool, Geophysical Research Letters, 33(20).

11.3

Shales retention properties and permeability through laboratory testing

Favero Valentina, Ferrari Alessio & Laloui Lyesse

Laboratory for Soil Mechanics, École Polytechnique Fédérale de Lausanne (EPFL), EPFL-ENAC-LMS, Station 18, CH-1015 Lausanne. (valentina.favero@epfl.ch; alessio.ferrari@epfl.ch; lyesse.laloui@epfl.ch)

The development of engineering activities involving shales such as the extraction of shale gas and shale oil, and the sequestration of CO_2, has led to an increasing need to understand the geomechanical behaviour of shales. The water retention mechanisms play a major role in fluid trapping due to the capillary forces present in low permeability formations as in the case of shale gas reservoir; moreover the variations in the degree of saturation (or suction) affect the swelling/shrinkage behaviour and the permeability of shales. Different techniques for the assessment of the retention properties are discussed. The first technique involves the direct control of the water content and the subsequent measurement of the suction at equilibrium by a psychrometer; a fluid displacement technique is used to detect the volume changes in order to allow the computation of the degree of saturation. The second procedure consists in progressive wetting and drying paths applied on a single shale sample and in the execution of psychometric readings in order to highlight hysteretical and scanning features in the retention behaviour.

Shale permeability and its relation to shale porosity are investigated by means of oedometric tests and direct permeability measurements.

Selected results are presented for three shales from Switzerland: the Opalinus Clay from the Mont Terri Underground Research Laboratory (URL), the "Brown Dogger" shale formation (depth of 766.67 - 807.44 m) and the Opalinus Clay formation (depth of 837.44 - 891.25 m), from a deep geothermal well near the village of Schlattingen in the Molasse Basin.

The water retention behaviour of the Opalinus Clay from Mont Terri is reported in Figure 1. The material has an initial degree of saturation close to one, which is in agreement with the fact that it was reported to be saturated in situ. The initial state was found along the main drying paths as a consequence of the coring process and the exposure to atmosphere before preservation. The main drying and wetting paths are well distinguished, and hysteresis zones can be observed. The evolution of the void ratios with the total suction showed that the porosity changes are more significant for the lowest range suction variations. The void ratios of the lowest measured suctions were in very good agreement with the results of the free swelling tests carried out with the same synthetic waters used for determining the water retention curves.

Shale permeability is assessed by means of laboratory testing: an advanced oedometric cell has been designed to investigate the volume change behaviour of shales at high vertical stresses and the permeability as a function of the vertical effective stress and porosity is computed by the back-analysis of the consolidation process. The previous results are compared to direct permeability measurements which are performed by means of an advanced triaxial system. High pressure gradients and high confining stresses are required in order to produce measurable flows. The good agreement of the obtained results can be highlighted and a clear decrease of shale permeability with decreasing porosity can be observed. The agreement of the obtained results shows that, when the end-of-primary consolidation and the coefficient of consolidation are properly computed, high-pressure oedometric tests can be used to gather information on the permeability of the tested shales within a significant range of porosity (Ferrari and Laloui, 2012).

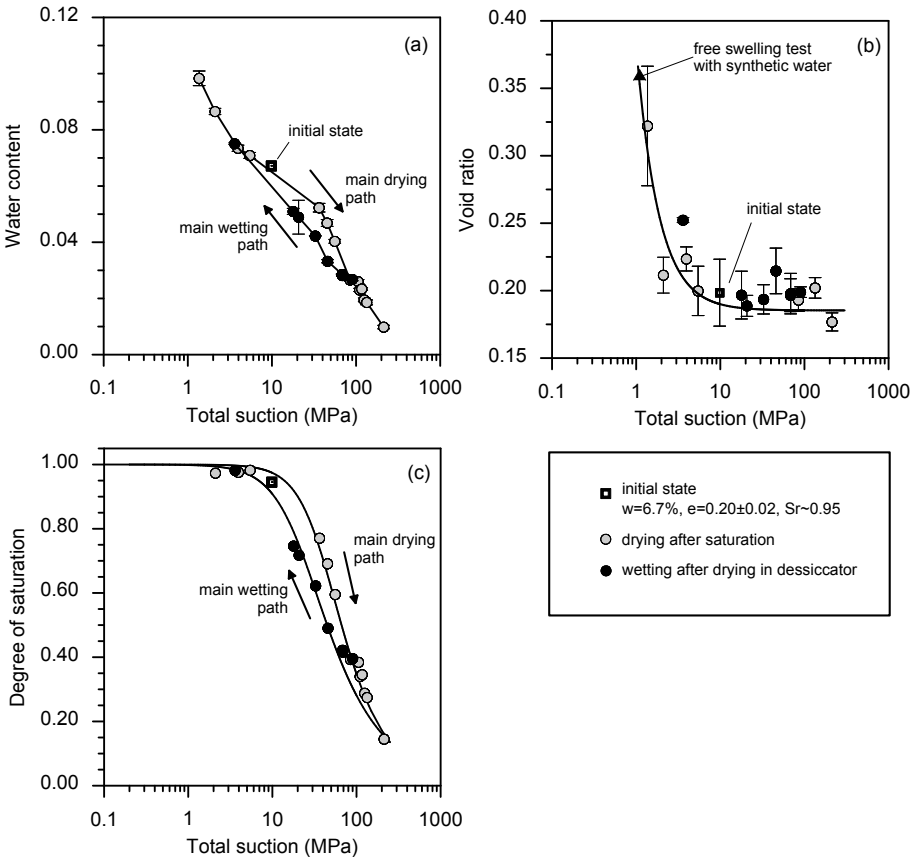

Figure 1. Water retention behaviour of the Opalinus Clay core sample: the water content (a), the void ratio (b) and the degree of saturation (c) as a function of the total suction.

REFERENCES

Ferrari, A. and Laloui, L. 2012: Advances in the testing of the hydro-mechanical behaviour of shales. In L. Laloui and A. Ferrari editors. Multiphysical Testing of Soils and Shales, pages 57-68, Springer.

11.4

High-resolution CMP-refraction seismics in combination with refraction tomography, reflection seismics and surface wave analysis

Hunfeld Ulrich[1], Brenner Olaf[2] & Orlowsky Dirk[2]

[1] *Wili 3, CH-6222 Gunzwil (Ulrich.Hunfeld@bluewin.ch)*
[2] *DMT GmbH & Co. KG, Exploration & Geosurvey, Am Technologiepark 1, D-45307 Essen*

Motivation
High-resolution seismic measurements were carried out in spring 2009 to evaluate the subsoil of a construction site. The results were used for the design of the tunnel system of a motorway in a urban area.

Aims
The aim of the study was to determine the exact position of the second refractor. There was a geological fault zone suspected in the second refractor and the location should be determined by the measurement.

Methods used
The data acquisition was carried out with three different seismic sources: The three sources were an accelerated drop weight (type Mjölnir), a sledgehammer of 8 kg and a vibroseismic air source. The signal quality of the different sources are compared. The receiver layout was a fixed spread layout with a geophone spacing of one meter and a source point spacing of two meters. This spread was chosen to fit each requirements of the selected data processing methods.

The seismic data was analysed with the methods of CMP-refraction, refraction tomography and reflection seismics. An analysis of the surface waves was also performed. Like the results of the reflection seismics, the results of the CMP-refraction seismics is also a stacked section with time to depth converted layer boundaries. In opposite to a standard refraction or a refraction tomography, the phase information of the seismic wave is also taken into account in the stacked section. Together with the wave velocity distribution in the refraction tomography section, the analysis of the surface waves and the deeper layer boundaries derived from the seismic reflection section, all information within the seismic data can be used in optimally manner.

Results
The results of each data processing methods are presented and compared. Figure 1 shows the interpreted section of the refraction tomography and Figure 2 the geological interpreted combined stacked section of the CMP-refraction and reflection seismics. Based on these results, the main focus of the discussion will be lying on the advantages of the common interpretation of the different methods.

Acknowledgement
The activities were carried out by DMT GmbH & Co. KG in spring 2009.
I would like to express my gratitude for using the results in this presentation.

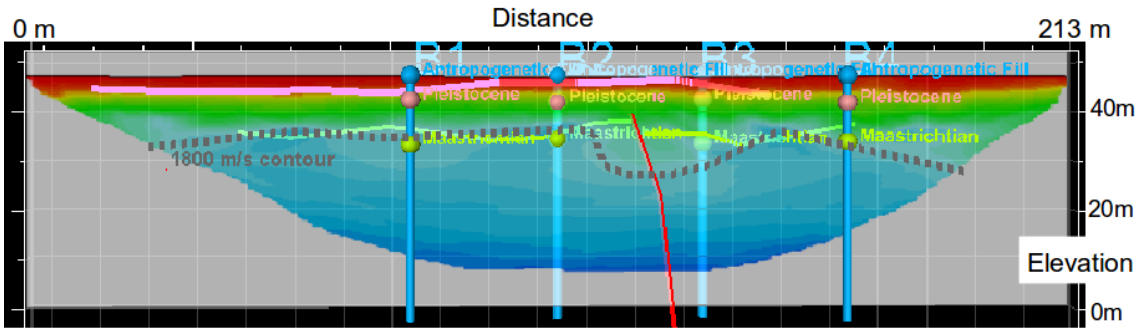

Figure 1. Interpreted section of the refraction tomography

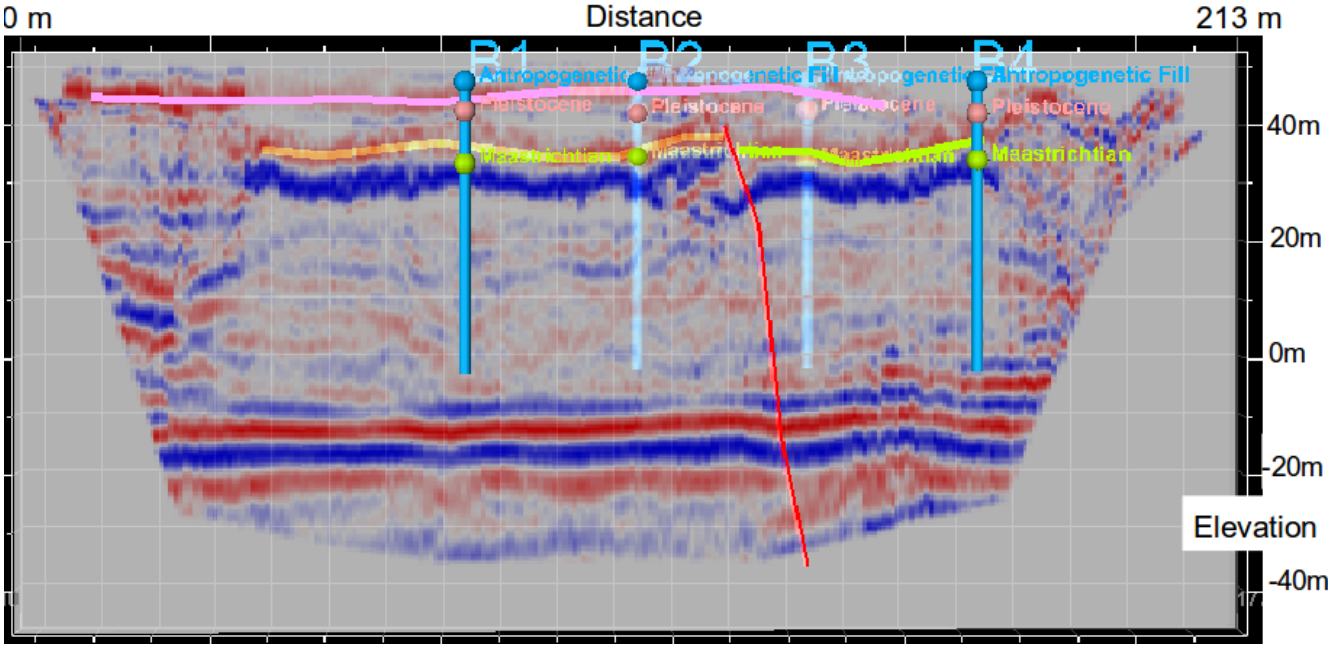

Figure 2. Geological interpreted combined stacked section of the CMP-refraction and reflection seismics

11.5

Seismoelectric effects due to mesoscopic heterogeneities: numerical study for a fractured rock

Jougnot Damien, Rubino J. German, Rosas Carbajal Marina, Linde Niklas, and Holliger Klaus

[1]*Applied and Environmental Geophysics Group, University of Lausanne, CH-1015 Lausanne, Switzerland.*

When a seismic wave propagates through a fluid saturated porous medium, it produces a relative motion between the fluid phase and the rock matrix. In the presence of an electric double layer at the fluid-solid interface, this movement introduces a separation of electrical charges which in turn generates a time-varying electrical source current and a resulting distribution of electrical potential (Pride, 1994). The presence of mesoscopic heterogeneities, that is, heterogeneities having sizes larger than the typical pore size but smaller than the prevailing wavelength, can induce a significant oscillatory fluid flow in response to the propagation of seismic waves (Müller et al., 2010). Indeed, the energy dissipation related to this phenomenon is considered to be one of the most common and important seismic attenuation mechanisms operating in the shallow part of the crust. Given that the amount of fluid flow produced by this phenomenon can be significant, a potentially important seismoelectric signal is also expected in such media. However, to the best of the authors' knowledge, the role played by mesoscopic wave-induced fluid flow on seismoelectric phenomenon is so far largely unexplored.

In this work, we propose a numerical approach for computing seismoelectric signals related to the presence of mesoscopic heterogeneities such as fractures. To this end, we consider a two-dimensional homogeneous sandstone sample containing three fractures with a small aperture. We apply an oscillatory compression on its top boundary considering a frequency range from 1Hz to 10kHz and an amplitude of 1kPa (Rubino et al., 2011). The solid phase is neither allowed to move on the bottom boundary nor to have horizontal displacements on the lateral boundaries and the fluid is not allowed to flow into or out of the sample. The fluid velocity field is determined by solving the quasi-static poroelastic equations in the space-frequency domain under the governing boundary conditions (Rubino et al., 2009). Next, the seismoelectric conversion is calculated using the so-called effective electrical excess charge approach, which has been recently developed in streaming potential studies (Revil et Leroy, 2004).

For the particular material properties and geometries considered in this analysis, the results clearly show a frequency-dependent response of the seismoelectric signal that is caused by the mesoscopic heterogeneities (Fig. 1). The magnitude tends to be negligible at frequencies below 100Hz. Conversely, at higher frequencies the induced fluid flow between the fractures and the embedding rock matrix becomes fairly important, thus yielding a measurable seismoelectric signal of a few mV. Our results therefore suggest that seismoelectric signals caused by mesoscopic heterogeneities should be explored in more detail. Such efforts should not only include further numerical analysis to better understand the role played by different types of heterogenities, but also well-controlled laboratory investigations.

REFERENCES

Jougnot, D., Rubino, J. G., Rosas Carbajal, M., Linde, N., & Holliger, K., 2013: Seismoelectric effects due to mesoscopic heterogeneities, Geoph. Res. Lett., 40, 2033–2037.

Müller, T., Gurevich, B., & Lebedev, M., 2010: Seismic wave attenuation and dispersion resulting from wave-induced flow in porous rocks – A review, Geophysics, 75, A147–A164.

Pride, S., 1994: Governing equations for the coupled electromagnetics and acoustics of porous media, Phys. Rev. B, 50, 15,678–15,696.

Revil, A. & Leroy, P., 2004: Constitutive equations for ionic transport in porous shales, J. Geoph. Res., 109, B03208.

Rubino, J. G., Ravazzoli, C., & Santos, J., 2009: Equivalent viscoelastic solids for heterogeneous fluid-saturated porous rocks, Geophysics, 74, N1–N13.

Rubino, J. G., Guarracino, L., Müller, T. M., & Holliger, K., 2013: Do seismic waves sense fracture connectivity? Geophys. Res. Lett., 40, 692–696.

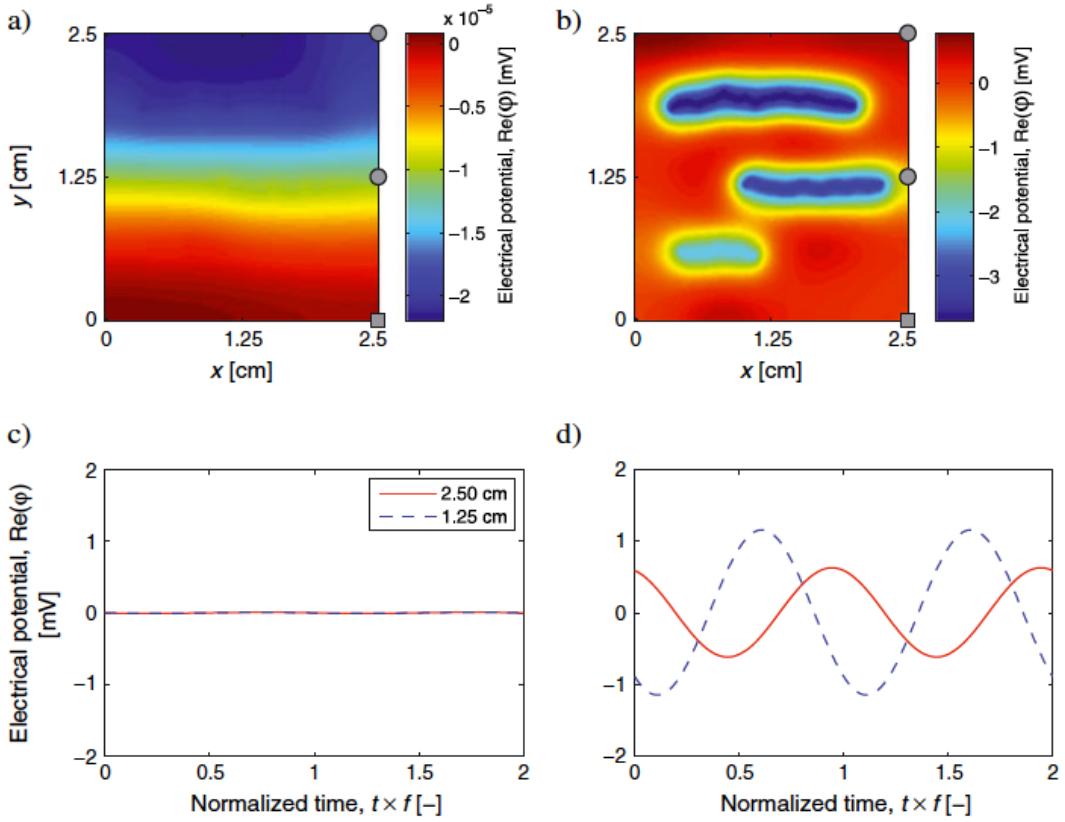

Figure 1. Seismoelectric potential response to the oscillatory compression test on a fractured sandstone for 1 Hz (a. & c.) and 10 kHz (b. & d.) (modified from Jougnot et al., 2013)

11.6

Focusing of seismic energy at LUSI mud volcano, Indonesia

Lupi, M., Saenger, E. H., Fuchs, F., Miller, S. A

1 ETH Zurich, Geological Institute, Sonnegstrasse 5, 8092, Zurich, CH
2 Steinmann Institute, University of Bonn, Meckenheimer Allee 173, Bonn, DE

The M6.3 Yogyakarta earthquake occurred offshore of Central Java on May 27th, 2006. Forty seven hours later, hot mud erupted approximately 250 km from the earthquake epicenter near Sidoarjo, Java. The continuous, and still on-going, eruption of mud orginated the LUSI mud volcano, which is the youngest mud volcanic system on earth. The causes that initiated the eruption are still debated and are based on different geological observations. The earthquake-triggering hypothesis is supported by the evidence that at the time of the earthquake ongoing drilling operations experienced a loss of the drilling mud down-hole. In addition, the eruption of the mud began only 47 hours after the Yogyakarta earthquake and the mud reached the surface at different locations aligned along the Watukosek fault, a strike-slip faults upon which LUSI resides. Moreover, the Yogyakarta earthquake also affected the volcanic activity of Mt. Semeru, located as far as Lusi from the epicentre of the earthquake. However, the drilling-triggering hypothesis points out that the earthquake was too far from LUSI for inducing relevant stress changes at depth and highlight how upwelling fluids that reached the surface first emerged only 200 m far from the drilling rig that was operative at the time. Hence, was LUSI triggered by the earthquake or by drilling operations?

A recent study suggests that a high-velocity seismic reflector located above the low-velocity formations that fed the mud eruption may have enhanced and focused seismic energy from the Yogyakarta earthquake and initiated the mud eruption. However, the occurrence of such a high-velocity formation at approximately 1000 m deep as well as the velocity model used to characterize the numerical study have been highly debated. To investigate effects of such a high-velocity layer and the sensitivity of the numerical analysis to the velocity model we conducted further simulations and found that the overall geological structure characterized by alternating and contrasting impedances, not the single high-velocity layer, is key to understand the response of the system and the resulting wave field.

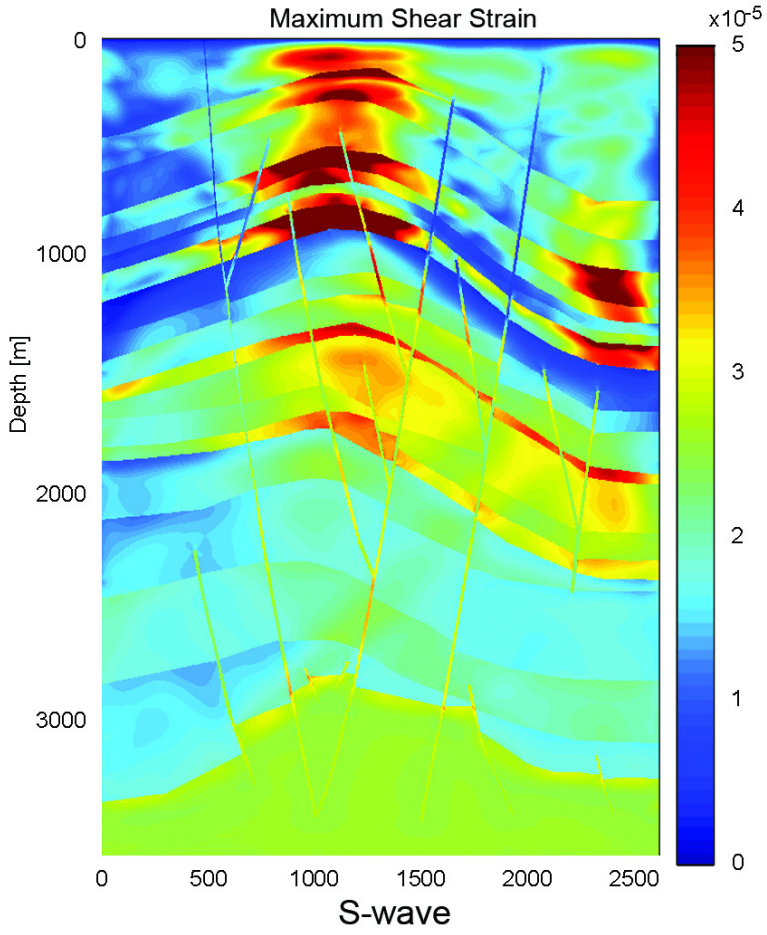

11.7

Assessment of the complex rock mass conditions for tunnels and underground caverns of the Hydropower Project Cerro del Águila (Peru)

Thüring Manfred & Sayah Selim M.

Lombardi Engineering Ltd., Via R. Simen 19, CH-6648 Minusio, Switzerland
(manfred.thuering@lombardi.ch, selim.sayah@lombardi.ch)

The project

The 510 MW hydropower project Cerro del Águila is currently under construction by Lombardi Ltd. as the designer, the consortium AGyM (Astaldi SA, Italy and Graña y Montero, Peru) as the constructor and KALLPA as the client. It is located in the external Peruvian Andes (Amazonian watershed) and exploits the water of Rio Mantaro. The plant consists of a 80 m high gravity dam, a roughly 5.7 km long headrace tunnel and 1.9 km long tailrace tunnel with a 93 m2 simplified horseshoe section, a powerhouse cavern of 40x86x18 m (height/length/width) located 350 m underground and various surge, access and adit tunnels. All underground excavations are carried out using the conventional drill and blast method.

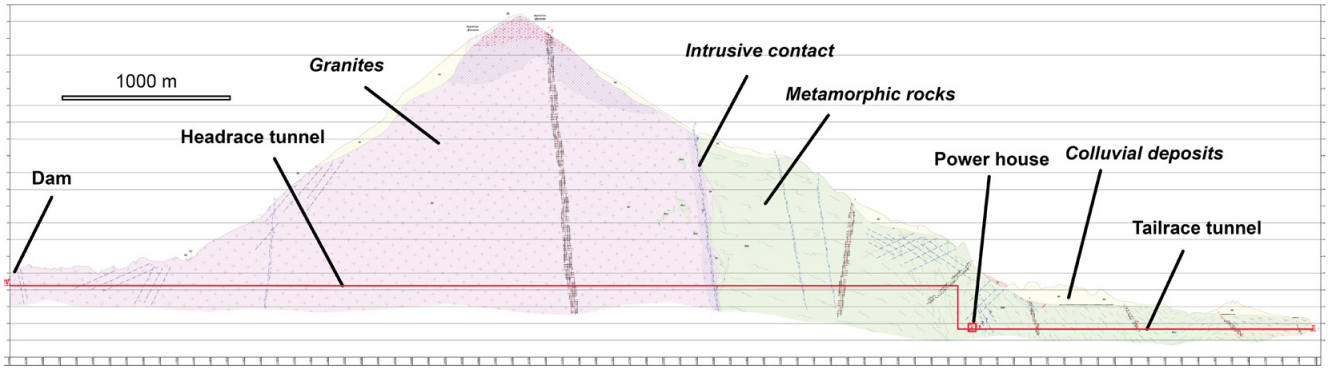

Figure 1: Geological profile along the 7.6 km long headrace-tailrace tunnel system.

Geological challenges

The project has several exceptional and challenging features (Figure 1):

The 7.6 km long headrace-tailrace tunnel of more than 10 m section height runs under a maximum overburden exceeding 1600 m in a mixed geological environment of highly metamorphic paragneisses intruded by granites, introducing the probable threat of rock burst and convergences. Particularly challenging will be the crossing of the intrusive contact under an overburden of 900 m.

Recent tectonics and uplift have created more than 125 m thick colluvial/landslide deposits, fracture patterns and a spectacular topography particularly at the powerhouse area, putting challenges for the construction of access roads and the condition of the rock mass for the excavation of the power house cavern and the tailrace tunnel.

The power house cavern is situated under a strongly inclined slope, 350 m below surface, demanding a special focus on the rock mass conditions and water tighting of the pressure shaft and alignment of the caverns with in-situ stresses and joints orientation. For this reason extensive hydrojacking tests were carried out in order to verify the initial geological assumptions related to the rock quality of the cavern system and the unlined pressure shaft.

Work progress

In order to better understand the underground conditions the geological model of the feasibility study has been completed by an investigation campaign, consisting of boreholes with field tests, seismics and laboratory tests for the key project structures. Together with geological field surveys the scheme was optimized.

Figure 2: Progress of excavation of more than 10 m high headrace tunnel, performed by drill and blast.

This presentation illustrates how the various geological and design related challenges concerning the rock mass condition have been addressed and resolved, using boreholes, field tests, seismic campaigns, hydrojacking tests, and computer modeling. A particular focus is put on the underground structures (tunnels and powerhouse cavern). The presentation also shows the current progress of the project (Figure 2).

11.8

Lowering microseismic detection threshold by sonogram analysis for Fribourg area (Switzerland)

Vouillamoz Naomi[1], Abednego Martinus[1], Deichmann Nicolas[2], Wust-Bloch Hillel Gilles[3], Mosar Jon[1],

[1]*University of Fribourg, Department of Geosciences, Earth Sciences, Chemin du Musée 6, CH-1700 Fribourg, Switzerland (martinussatiapurwadi.abednego@unifr.ch, naomi.vouillamoz@unifr.ch, jon.mosar@unifr.ch).*
[2] *Schweiz. Erdbebendienst (SED), Sonneggstrasse 5, CH-8092 Zürich, Switzerland*
[3] *Tel Aviv University, Department of Geophysics and Planetary Sciences, P.O.B. 39040, Tel Aviv, 69978, Israel*

This study investigates low-magnitude seismicity generated within the Fribourg area (Western Molasse Basin – Switzerland (Fig 1)). It focuses on the Fribourg Lineament (FL), a North-South trending cluster of weak earthquakes that were generated East of the city of Fribourg and may be associated to the lineament described by Kastrup et al. (2007). Visual event screening by sonogram analysis (Sick et al. 2012) is carried out on 50 months of continuous data recorded by the Swiss Earthquake Service (SED), between 2001 and 2013.

Earthquake detection is carried out with the NanoseismicSuite software package (Institute for Geophysics-Stuttgart: Joswig 2008; Sick et al. 2012), which uses sonograms, a type of power spectral density (PSD) matrix. These PSD, which are noise adapted, muted and pre-whitened, allow for the detection of signal energy near to 0 dB signal to noise ratio (SNR).

This analysis uses continuous data recorded between October 2001 and April 2013 by three SED permanent stations: SCOU, STAF and TORNY (Figure 1). SCOU and STAF are two accelerometers installed in 2008 at some 5 and 10 kilometers away from the FL. TORNY is a broadband sensor located 20 kilometers west of the FL (Figure 1), whose continuous data is available since 2001.

The ECOS-09 catalog (Earthquake Catalog of Switzerland) reports about 40 events recorded between 2001 and 2012, within a radius of 20 km around the city of Fribourg. Our sonogram-based analysis of SED continuous data for the same period and same area, identified more than 200 previously undetected events.
Among these 200 events, 60 can be reliably located with the NanoseismicSuite software, using SED waveforms recorded near the FL as well as data acquired by two mini-arrays deployed near the FL (Abednego & Vouillamoz, 2011). The remaining micro-earthquakes do not present enough phase information to be located. Since most of these weaker events show excellent signal correlation (>90%) with higher magnitude events, they have been used for further earthquake spatio-temporal analysis. Our new catalog shows how most of the 200 events can be associated to specific event clusters along the FL.

Our analysis suggests that most events, which were newly detected, are indeed located on the FL and seem to be related to stronger earthquakes that were previously detected (Kastrup et al., 2007). However, our new catalog shows that additional events, previously undetected, cluster under the city Fribourg. Since these events are not located near substructures that were detected and interpreted by existing subsurface imaging surveys (Interoil 2010), our investigations show the potential of sonogram analysis for active fault mapping and seismic hazard assessment.

REFERENCES

Abednego, M. & Vouillamoz, N., Wust-Bloch H. G., Mosar J., 2011. Nano-seismology on the Fribourg Lineament - Switzerland. Poster presented at the Swiss Geoscience Meeting 2011, Zürich.

Interoil, 2010. 2D Seismik Interpretation in den Gebieten Payerne, Fribourg und Berner Seeland. Bercicht vorbereitet von Interoil E&P Switzerland AG für die Resun AG, Zürich, September 2010.

Joswig, M., 2008. Nanoseismic monitoring fills the gap between microseimic networks and passive seismic, First Break, 26, 2008.

Kastrup, U., Deichmann, N., Fröhlich, A., Giardini, D., 2007. Evidence for an active fault below the northwestern Alpine foreland of Switzerland, Geophys. J. Int. (2007) 169, 1273-1288.

Sick, B., Walter, M., Joswig, M., 2012. Visual Event Screening of Continuous Seismic Data by Supersonograms, Pure Appl. Geophys., 2012.

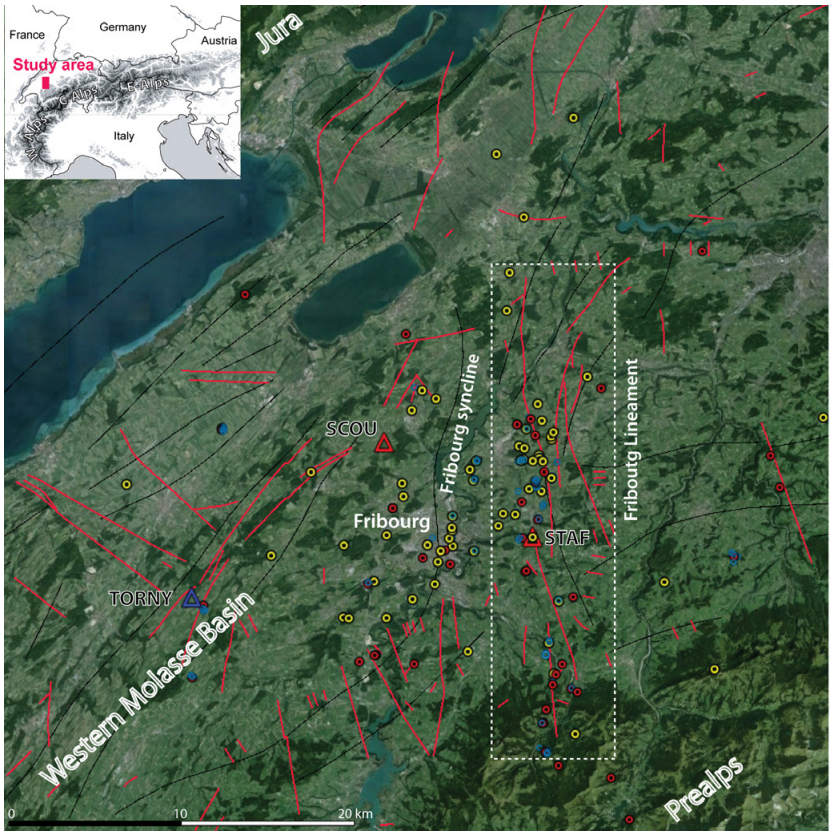

Swiss permanent networks (SED-Swiss seismological service)

- Digital broadband seismometers SDSNet Streckeisen STS-2
- Strong Motion accelerometers SSMNet Kinemetrics EpiSensor

Structure

- Faults, interpreted from seismic lines (Interoil, 2010)
- Major fold axis in the Western Molasse Basin

Earthquake Catalog

- ECOS-09 events located with the Nanoseismic-Suite software package
- Events undetected by SED, reliably located with the NanoseismicSuite software package
- Events undetected by SED, presenting correlation factor higher than 90 % with related master event and co-located with the NanoseismicSuite software package

Figure 1: Google Earth view of study area with location of SED permanent stations used for earthquake detection, principal tectonic structures and earthquake catalog.

P 11.1

Large mass wasting deposits in Lake Geneva off the city of Lausanne revealed by detailed reflection seismic data

Correia-Demand Jehanne[1], Marillier François[1], Kremer Katrina[2,3] & Girardclos Stéphanie[2,3]

[1]*Center for Research on Terrestrial Environment (CRET), University of Lausanne, Geopolis, CH-1015 Lausanne (jehanne.correia-demand@unil.ch)*
[2]*Department of Earth Sciences, University of Geneva, Rue des Maraîchers 13, CH-1205 Genève*
[3]*Environmental Sciences Institute (ISE), University of Geneva, Site Batelle, Route de Drize 7, CH-1227 Carouge*

Seismic studies in the central part of Lake Geneva ("Grand-Lac") have revealed the occurrence of several mass wasting deposits (MWD) within Holocene sedimentary layers. While some of them are small, a large MWD (MWD A) is observed off the city of Lausanne. The depth of the associated failure scars (100 m water depth), its volume (~ 13 km^3), and the occurrence of other smaller MWD's that were possibly co-deposited with MWD A point to a major event in the lake, most likely associated with an earthquake. Numerical simulations indicate that it could have generated a tsunami with local wave heights of up to 6 m near Lausanne. This earthquake-triggered event may be responsible for a gap in lake-dweller occupation in this region revealed by dendrochronological dating of remaining piles at palafitte sites (Kremer et al, in review).

To resolve the details of the MWD offshore Lausanne and to better understand its geological context different seismic systems were used. These were a 3.5 KHz pinger with a theoretical vertical resolution of 0.15 m and a multichannel system with either a water gun or an air gun seismic source with vertical resolution of 0.6 m and 1.1 m, respectively. After a first pass processing, the water gun data were reprocessed in order to take into account the shape of the streamer in the water. Examples of the different seismic resolutions as well as the enhanced data quality through reprocessing are shown in Figs. 1 to 4.

In addition to typical seismic images of MWDs often observed in other alpine lakes, intriguing features within the Holocene sediments with apparent sub-vertical offsets are shown in both the water-gun and pinger seismic data (Figs. 2 to 4). They are located above large faults zones in the Tertiary Molasse. The question whether these features and the large MWD off Lausanne were caused by the activity of these faults must be further investigated.

REFERENCE

Kremer, K., Marillier, F., Hilbe, M., Simpson, G., Dupuy, D., Yrro, B., Rachoud-Schneider, A-M., Corboud, P., Bellwald, B., Wildi, W. & Girardclos, S..Pile dwellers occupation gap in Lake Geneva (France-Switzerland) possibly explained by an earthquake – slide – tsunami event during Early Bronze Age. In review at Earth and Planetary Science Letters.

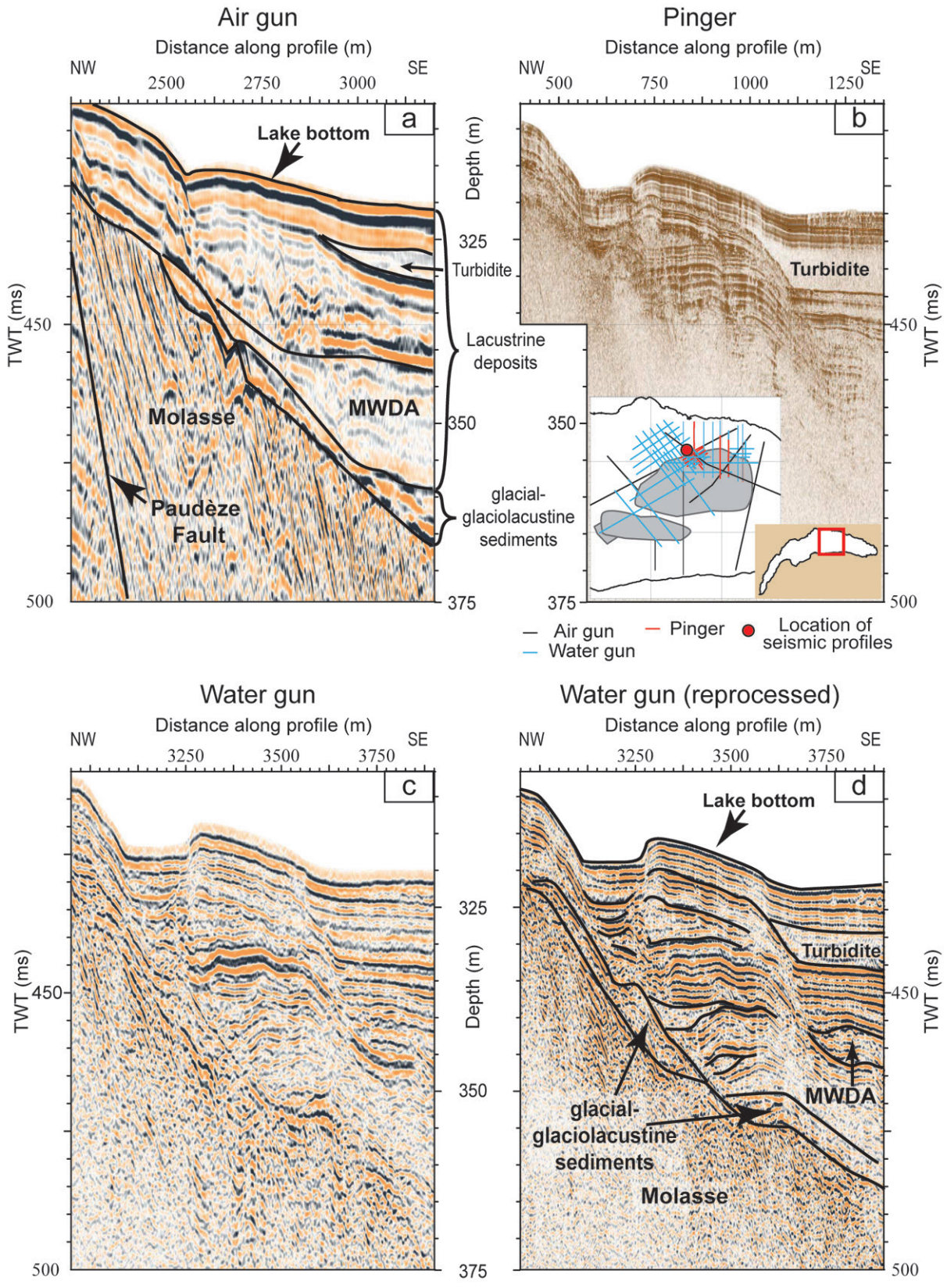

Figure 1. Comparison of seismic profiles with different seismic sources or processing. b), c) and d) show profiles with identical locations. a) Profile with orientation slightly different from the other ones, but sampling the same geological structures. Simplified geological interpretation shown on a) and d). MWDA : Mass-wasting deposit off the city of Lausanne.

P 11.2

Modeling Electric Current Flow in 3D Fractured Media

Serdar Demirel, Delphine Roubinet, and James Irving

Applied and Environmental Geophysics Group, Center for Research of the Terrestrial Environment, University of Lausanne, Switzerland

The study of fractured rocks is highly important in a variety of research fields and applications such as hydrogeology, geothermal energy, hydrocarbon extraction, and the long-term storage of toxic waste. Fractured media are characterized by a large contrast in permeability between the fractures and the rock matrix. For hydrocarbon extraction, the presence of highly conductive fractures is an advantage as they allow for quick and easy access to the resource. For toxic waste storage, however, the fractures represent a significant drawback, as there is an increased risk of leakage and migration of pollutants deep into the subsurface. In both cases, the identification of fracture network characteristics is a critical, challenging, and required step.

Recently, we have utilized the discrete fracture network (DFN) approach to model electric current flow in 2D fractured media. Our approach is based on a discrete dual-porosity model where fractures are represented explicitly, the matrix is coarsely discretized into blocks, and current flow exchange between the fracture and matrix is analytically evaluated at the fracture scale and integrated at the block scale. This approach is promising and has proven its efficiency for 2D simulations. However, its extension to 3D fractured media is a challenge that remains to be addressed. Assuming that fractures can be represented by two-dimensional finite planes embedded in a surrounding matrix, the principal difficulties are (i) expressing current flow conservation at fracture intersections that are represented by lines in 3D, instead of by nodes in 2D; (ii) evaluating the impact of fracture-matrix exchange at the fracture scale on the electric potential in a fracture; and (iii) integrating the fracture-matrix exchange from the fracture scale to the matrix-block scale in order to evaluate its impact on the electric potential in the porous domain.

We are working on developing an efficient model for electric current flow in 3D fractured rock with the following main application objectives: (i) studying the impact of heterogeneous fracture orientations, as existing 3D solutions are analytical and deal only with horizontal and vertical fractures; and (ii) applying our model to large-scale fracture networks that provide major pathways for electric current, as existing 3D numerical methods would underestimate these effects by integrating fracture electrical conductivity to a block-scale equivalent conductivity. The overarching goal of our work is to test how geoelectrical surveys may help with localizing and characterizing fractures in natural environments through a low-computational-cost modeling method.

P 11.3

Exploring the Issue of Model Error in Stochastic Solutions to Hydrogeophysical Inverse Problems

Corinna Koepke, James Irving, and Delphine Roubinet

Applied and Environmental Geophysics Group, Center for Research of the Terrestrial Environment, University of Lausanne, Switzerland

Geophysical methods have gained much interest in hydrology over the past two decades because of their ability to provide, in a minimally invasive manner, estimates of the spatial distribution of subsurface properties at a scale that is often relevant to key hydrological processes. Because of an increased desire to quantify uncertainty in hydrological predictions, many hydrogeophysical inverse problems have recently been posed within a Bayesian framework, such that estimates of hydrological properties and their corresponding uncertainties can be obtained. With the Bayesian approach, it is often necessary to make significant approximations to the associated hydrological and geophysical forward models such that stochastic sampling from the posterior distribution, for example using Markov-chain-Monte-Carlo (MCMC) methods, is computationally feasible. These approximations lead to model structural errors in the inverse problem which, if not properly accounted for through the Bayesian likelihood function, have the potential to influence posterior parameter estimates and uncertainties to the extent that subsequent hydrological predictions become meaningless. So far, however, the characterization and proper treatment of model errors in hydrogeophysical inverse problems has not been investigated.

Here, we present initial work in this domain with reference to the inverse problem of estimating unsaturated hydraulic properties, namely the van Genuchten – Mualem parameters, in a series of subsurface layers from time-lapse, zero-offset-profile (ZOP), ground penetrating radar (GPR) data collected over the course of an infiltration experiment. In particular, we investigate stochastically the effect of a variety of assumptions, commonly made for the sake of computational tractability during the stochastic inversion of these data, on the errors produced in the modeled results as a function of depth and time. These assumptions include (i) that infiltration is purely vertical and can thus be modeled by the one dimensional Richards' equation; (ii) that the subsurface layers are internally homogeneous; and (iii) that the infiltration rate of water into the subsurface is exactly known. Results so far indicate that model errors for this problem are far from being normal and independently identically distributed, which has been the common assumption in all previous stochastic inversion efforts in this domain. As a result, posterior uncertainties obtained through these efforts will likely be strongly biased. Future work will involve developing more appropriate likelihood functions to be used in Bayesian-MCMC inversions, with the goal of obtaining more meaningful posterior parameter estimates and uncertainties.

P 11.4

Improvement of the regional 3D modeling of deep geological structures with gravity: A case study in the Neuchatel Jura Mountains.

Kuhn Pascal[1], Abdelfettah Yassine[2], Mauri Guillaume[3], Schill Eva[4,5] & Vuataz Francois-David[2]

[1] *Eidgenössisches Departement für Verteidigung, Bevölkerungsschutz und Sport VBS, armasuisse, Bundesamt für Landestopografie swisstopo, Landesgeologie, Seftigenstrasse 264, CH-3084 Wabern (pascal.kuhn@swisstopo.ch)*
[2] *Centre for Hydrogeology and Geothermics (CHYN), University of Neuchâtel, Emile-Argand 11, CH-2000 Neuchâtel (yassine.abdelfettah@unine.ch)*
[3] *Geo2X SA, Oulens-sous-Echallens, CH-1377*
[4] *EEIG «Heat Mining», Route de Soultz - BP 40038, F-67250 Kutzenhausen, France*
[5] *Steinbeis-Transfer Centre «Geoenergy and Reservoir Technology» D-79807 Lottstetten-Nack, Germany*

Pioneer work on the Atlas of gravimetry (Klingelé & Olivier, 1980) has allowed the scientific community to discover that the underground structure of Switzerland was affected by significant gravity variation within the Molasse basin, the Rhine graben and the Jura Mountains. While some of the gravity decreases are clearly associated to sedimentary deposit during the post-Mesozoic period, source of decrease of gravity in other parts cannot be explained using the existent knowledge on current geophysical and geological information. Post processing of the Bouguer anomaly allows an interpretation of the density anomalies correlating with the deep Paleozoic structures (Abdelfettah et al., in preparation). Permo-Carboniferous basins has been identified in seismic studies (Sommaruga et al., 2012) as well as in former gravity explorations (Klingelé & Schwendener, 1984).

A gravity data set from the BRGM was also used to cover the French area. Special considerations were taken in account to merge both Swiss and the French database. Two techniques were used to validate this compilation; i) using a geostatistical approach, and ii) using the means value of the neighboring measurements within a specified radius. In the end, a complete Bouguer anomaly computed at the same ellipsoid is obtained for the whole studied area. As this Bouguer anomaly is strongly dominated by the regional trend, caused by the sedimentary layer and by the deepening of the crystalline basement, a Betterworth filter (Abdelfettah and Schill, 2012) using different wavelengths was applied to get residual anomalies which are ready to be interpreted.

This study investigates the occurence of Permo-Carboniferous basins underneath the Jura Mountains in the north-west part of Canton of Neuchâtel. The investigated area reaches from Pontarlier (F) in the west to Biel/Bienne in the east as well as Estevayer-le-Lac in the south to Orasans (F) in the north resulting in a geological 3D model of ~65x50 km. Due to the regional scale and the low data-density (geological profiles, seismics, drillholes) the model was set up using 13 geological profiles (Charrue unpubl.; Pfiffner, 2009; Sommaruga et al., 2012) and 3 deep drillholes. The obtained 3D geological model has then been used to calculate the theoretical gravity response by doing a 3D forward modeling. By try and error the modeled structures must fit the real gravity data as close as possible.

A comparison of the observed gravity data with the gravity model response reveals that to reduce the misfit, a density variation of the Permo-Carboniferous basins in the Paleozoic basement must be considered.

REFERENCES

Abdelfettah Y., Schill E., Kuhn P., in preparation. Characterization of geothermally relevant inhomogeneities in crystalline basement using filters and gravity forward modeling: an example from to Permo-Carboniferous grabens in Switzerland.

Abdelfettah Y. & Schill E., 2012. Delineation of geothermally relevant Paleozoic graben structures in the crystalline basement of Switzerland using gravity. Submitted to Society of Exploration Geophysics meeting, Istanbul, 2012.

Klingelé, E. and Olivier, R., 1980. Die neue Schwere-Karte der Schweiz (Bouguer- Anomalien), Bern.

Klingelé, E. & Schwendener H., 1984. Geophysikalisches Untersuchungsprogramm Nordschweiz: Gravimetrische Messungen 81/82, Nagra, Baden.

Sommaruga, A., 1997. Geology of the central Jura and the molasse basin: New insight into an evaporite-based foreland fold and thrust belt. Dissertation. Univ. Neuchâtel.

Sommaruga A., Eichenberger U. & Marillier F., 2012. Seismic Atlas of the Swiss Molasse Basin. 24 Tafeln. ISBN 978-3-302-40064-8.

P 11.5

Laboratory seismic scale model study of reflection imaging beneath a distorting near surface zone

Yike Mo & Hakki Karaman

[1]*Institute of Geophysics, ETH Zürich, Sonneggstrasse 5, CH-8092 Zürich (yimo@student.ethz.ch)*

The near-surface weathered layer has a profound impact on surface seismic reflection data (Yilmaz, 2001). Surface waves, guided and refracted waves often obscure the reflection record, especially when near surface layering is present and the velocity contrasts are strong. Unfortunately, our understanding of the physics of wave propagation in the near surface is limited and the techniques available to invert for near-surface properties have not been developed to a stage where they can be applied to solve many relevant problems.

To tackle the challenges and imaging problems referred to above, several two – dimensional scale models built out of 2 mm thick plastic and metal sheets (cut and bonded together) were assembled in the Wave Propagation Lab at ETH Zurich. The models were used, in full recognition of the similitude relations (Pant et al., 1988), to investigate reflections from beneath a complex overburden. The plate models are rather thin relative to a wavelength, so that the only longitudinal and shear waves which propagate in the plate are the fundamental mode symmetric non-dispersive vibrations which travel at the plate velocity V_p and the extended medium shear velocity β, respectively (Redwood, 1960). Dipping layers, anomalous block inserts were simulated. The experiment entails the use of a piezoelectric source driven by a pulse amplifier at ultrasonic frequencies (20 – 300 kHz) to generate waves in the plate, which are detected by piezoelectric receivers and recorded digitally on a 32 channel National Instruments recording system, under SignalExpress software control.

In the experiment, a single cycle sinusoidal pulse with a negative onset (5 µs pulse width and 600 V pulse voltage) was selected as the optimized source. Reflection and transmission data were initially collected over a homogenous model for calibration purposes. For the heterogeneous models, different recording configurations and processing techniques, such as deconvolution, normal move-out and migration, were applied. The experiments are continuing but preliminary results clearly show the difficulties of imaging beneath an irregular overburden.

REFERENCES

Pant, D.R., Greenhalgh S. A. & Watson, S. 1988: Seismic reflection scale model facility. Exploration Geophysics. 19, 499–512.

Redwood, M. 1960: Mechanical Waveguides: The Propagation of Acoustic and Ultrasonic Waves in Fluids and Solids with Boundaries. 300 pp, Pergamon Press.

Yilmaz, Oz. 2001: Seismic Data Analysis: Processing, Inversion and Interpretation. Society of Exploration Geophysicists.

P 11.6

Material softening as a potential cause for the development of boudinage - an elasto-visco-plastic numerical modeling approach

Peters Max[1], Poulet Thomas[2], Karrech Ali[3], Regenauer-Lieb Klaus[4] & Herwegh Marco[1]

[1]*Institute of Geological Sciences, University of Bern, Switzerland*
[2]*CSIRO Earth Science and Resource Engineering, Kensington, Western Australia*
[3]*School of Civil and Resource Engineering, The University of Western Australia*
[4]*School of Earth and Environment, The University of Western Australia*

Layered rocks deformed under viscous deformation frequently show boudinage, a process which results from differences in effective viscosity between the layers involved (Goscombe et al., 2004 and references therein). Information on the deformation processes, physical conditions (T, stress, strain rate) and effective viscosities are crucial to obtain rheological constraints directly from nature. In the past, various numerical modeling studies of boudinage in layers under going power-law creep attempted to describe the development of pinch-and-swell structures under different physical deformation conditions (low to high T; e.g. Schmalholz and Maeder, 2012). However, there exists rather limited knowledge about both the origin of necking instabilities as well as the relation between boudinage and the involved flow regimes.

The finite element modeling software ABAQUS in combination with user-defined subroutines UMAT (Karrech et al., 2011a) was applied to investigate aforementioned problems. We implemented thermo-mechanical coupling between elastic, viscous and plastic deformation of pure calcite (Cc) or quartz (Qtz) aggregates or Qtz+Cc mixtures. Finite elements, each representing a population density function of a number of individual grains, undergo layer-parallel extension, which resembles co-axial plane strain. In terms of geometry, a simulated pure-shear box is built up by 3 layers, consisting of a central layer of coarse-grained populations, surrounded by finer grained populations on bottom and top. In contrast to previous studies, the rheology evolves with increasing shear strain starting with initial elastic behavior, adding then the transient Ramberg-Osgood strain hardening on the way to composite viscous flow (Herwegh et al., in review). Composite flow on the base of dislocation and diffusion creep for both mineral phases is involved.

Compared to nature, this model setup corresponds to a secondary phase-controlled polymineralic host rock (pinned and fine-grained matrix grains) around a coarse-grained monomineralic vein, in which grains can dominantly deform in a plastic manner involving dynamic recrystallization. While the small grain sizes in top and bottom layers are strain invariant, they are allowed to adapt to the physical deformation conditions in the central layer by grain growth or grain size reduction following an energy optimization procedure based on the Paleowattmeter approach of Austin and Evans (2007) and the thermodynamic approach of Regenauer-Lieb and Yuen (XYZ2004).

Note that the chosen model set up corresponds to situations in natural high strain shear zones such as thrust and detachment faults, where highly strained and fine grained polymineralic (ultra-) mylonites are subjected to synkinematic veining. We use natural examples of the Helvetic Alps and the Penninic front to check and discuss the relevance of our numerical results.

REFERENCES

Austin, N. and Evans, B. (2007). Paleowattmeters: A scaling relation for dynamically recrystallized grain size. Geology, 35.

Goscombe, B.D., Passchier, C.W. and Hand, M. (2004). Boudinage classification: End-member boudin types and modified boudin structures, Journal of Structural Geology, 26.

Herwegh, M., Poulet, T., Karrech, A. and Regenauer-Lieb, K. (in review). From transient to steady state deformation and grain size: A thermodynamic approach using elasto-visco-plastic numerical modeling. Journal of Geophysical Research.

Karrech, A., Regenauer-Lieb, K. and Poulet, T. (2011a). A Damaged visco-plasticity model for pressure and temperature sensitive geomaterials. Journal of Engineering Science 49.

Regenauer-Lieb, K. and Yuen, D. (2004). Positive feedback of interacting ductile faults from coupling of equation of state, rheology and thermal-mechanics. Physics of the Earth and Planetary Interiors, 142.

Schmalholz, S.M. and Maeder, X. (2012). Pinch-and-swell structure and shear zones in viscoplastic layers. Journal of Structural Geology, 34.

P 11.7

Two-dimensional probabilistic inversion of plane-wave electromagnetic data

M. Rosas Carbajal[1], N. Linde[1], T. Kalscheuer[2], J. Vrugt[3,4]

[1] *Applied and Environmental Geophysics Group, University of Lausanne (marina.rosas@unil.ch).*
[2] *Institute of Geophysics, ETH Zurich.*
[3] *Department of Civil and Environmental Engineering, University of California Irvine, 4130 Engineering Gateway, Irvine, CA 92697-2175, USA.*
[4] *Institute for Biodiversity and Ecosystems Dynamics, University of Amsterdam, Amsterdam, The Netherlands.*

Probabilistic inversions based on Markov chain Monte Carlo (MCMC) methods help to characterize the inherent non-uniqueness of non-linear inverse problems. By stating the inverse problem as an inference problem, the emphasis is placed on sampling the posterior probability density function (pdf) of the model parameters, which provides direct information about the model parameters' uncertainty. Unfortunately, for non-linear problems involving many model parameters, MCMC algorithms may take great time to converge. This is why most geophysical applications based on MCMC rely on 1D assumptions. We present here the first fully two-dimensional pixel-based MCMC inversion of radio magnetotelluric (RMT) and electrical resistivity tomography (ERT) data, using up to 300 model parameters. Using synthetic data, we demonstrate that stochastic inversion of high-dimensional problems necessitates prior constraints on the model structure to yield meaningful results. We investigate how model parameter uncertainty depends on model structure constraints using different norms of the likelihood function and on the model constraints. In particular, we focus on two popular types of regularization: smoothly varying model parameters and compact anomalies. We invert not only for the pdf of the model parameters, but also for two hyper-parameters: the variance of the data errors and a trade-off between data fit and model structure. The derived model uncertainties are compared with deterministic most-squares inversions and we analyze how these uncertainties change when jointly inverting RMT and ERT data. Finally, we present a field application to characterize the geometry of an aquifer in Sweden. The numerical examples illustrate that model regularization not only decreases the uncertainty of the model parameters, but also accelerates the convergence of the MCMC algorithm. A drawback is that the regularization may lead to posterior pdfs that do not contain features in the true model that are insensitive to data. This problem can be partly mitigated if the plane-wave EM data is augmented with ERT observations. The hierarchical Bayesian inverse formulation used is able to recover the probabilistic properties of the measurement data errors and a model regularization weight. Application of the proposed inversion methodology to field data from an aquifer demonstrates that the posterior mean model realization is very similar to that derived from a deterministic inversion with similar model constraints.

P 11.8

Discrete Dual Porosity Modeling of Electrical Current Flow in Fractured Media

Roubinet Delphine & Irving James

Center for Research of the Terrestrial Environment, University of Lausanne, Switzerland

The study of fractured rocks is highly important in a variety of research fields and applications such as hydrogeology, geothermal energy, hydrocarbon extraction, and the long-term storage of toxic waste. Fractured media are characterized by a large contrast in permeability between the fractures and the rock matrix. For hydrocarbon extraction, the presence of highly conductive fractures is an advantage as they allow for quick and easy access to the resource. For toxic waste storage, however, the fractures represent a significant drawback, as there is an increased risk of leakage and migration of pollutants deep into the subsurface. In both cases, the identification of fracture network characteristics is a critical, challenging, and required step.

A number of previous studies have indicated that the presence of fractures in geological materials can have a significant impact on geophysical electrical resistivity measurements. It thus appears that, in some cases, geoelectrical surveys might be used to obtain useful information regarding fracture network characteristics. However, existing geoelectrical modeling tools and inversion methods are not properly adapted to deal with the specific challenges of fractured media. This prevents us from fully exploring the potential of the method to characterize fracture network properties. We thus require, as a first step, the development of accurate and efficient numerical modeling tools specifically designed for fractured domains.

Building on the discrete fracture network (DFN) approach that has been widely used for modeling groundwater flow in fractured rocks, we have developed a discrete dual-porosity model for electrical current flow in fractured media. Our novel approach combines an explicit representation of the fractures with fracture-matrix electrical flow exchange at the block-scale. Tests in two dimensions show the ability of our method to deal with highly heterogeneous fracture networks in a highly computationally efficient manner, which permits us to study the impact of fractures and their properties on the electrical response of the domain. With additional development, the method will be extended to three dimensions and used in the context of geoelectrical field investigations.

P 11.9

Seismic energy dissipation in fractured rocks

J. Germán Rubino[1], Tobias M. Müller[2], Luis Guarracino[3] & Klaus Holliger[1]

[1] *Applied and Environmental Geophysics Group, University of Lausanne, CH-1015 Lausanne (German.Rubino@unil.ch)*
[2] *Earth Science & Resource Engineering Division, Commonwealth Scientific and Industrial Research Organization, Perth, Australia*
[3] *CONICET – Facultad de Ciencias Astronómicas y Geofísicas, Universidad Nacional de La Plata, Argentina.*

Up until now, the enhanced energy dissipation observed in fractured rocks has been considered to be mainly produced by wave-induced fluid flow (WIFF) between fractures and the pore space of the embedding matrix (e.g., Brajanovski et al., 2005). Since this process is strongly controlled by the hydraulic characteristics of the heterogeneous sample, it is expected that seismic attenuation also contains information on fracture connectivity.

Extending a recent pilot study of this topic (Rubino et al., 2013a), we explore here the effects of fracture connectivity on seismic attenuation. We represent fractures as highly compliant and permeable heterogeneities embedded in a stiffer porous matrix (e.g., Brajanovski et al., 2005) and employ a numerical upscaling procedure similar to that presented by Rubino et al. (2013b). That is, we apply an oscillatory compression at the top boundary of a square rock sample containing mesoscopic fractures. The solid phase is allowed neither to move on the bottom boundary nor to have horizontal displacements on the lateral boundaries. The fluid is not allowed to flow into or out of the sample. The equivalent undrained, complex plane-wave modulus, which contains the information on seismic attenuation for vertically propagating P waves, is expressed in terms of the applied compression and the oscillatory volume change. The latter is obtained by numerically solving the Biot's (1941) consolidation equations.

We consider two models corresponding to homogeneous water-saturated sandstones permeated by two quasi-orthogonal fractures without and with intersection (Figure 1). In both cases, the rock sample is a square of side length 3.33 cm, and the mean aperture of the fractures is 0.033 cm. The red curve in Figure 1 shows that the presence of fractures perpendicular to the direction of wave propagation produces strong attenuation over a wide frequency range. This is expected, because the strong compressibility contrast between the quasi-horizontal fracture and background material produces a large amount of fluid flow between these two regions and, consequently, energy dissipation. By comparing the blue and red curves we see that when the fractures intersect significant changes in the overall attenuation arise. In particular, the attenuation levels corresponding to WIFF between fractures and background material decrease and a second peak arises at higher frequencies. Corresponding spatial distributions of energy dissipation allow us to observe that in absence of fracture connectivity energy dissipation takes place in the vicinity of the quasi-horizontal fracture. In presence of fracture connectivity, dissipation takes place in the vicinity of the two fractures for the frequency of the first attenuation peak. However, the pressure gradient between fractures and background is reduced, and therefore the total energy dissipation is less significant (blue curve in Figure 1). For the frequency of the second attenuation peak, 98% of the energy dissipation takes place inside the connected fractures, thus demonstrating that this additional peak is due to WIFF within the fractures. That is, the applied compression at the top boundary of the sample induces a strong fluid pressure increase in the quasi-horizontal fracture. This, in turn, generates fluid injection from the horizontal fracture into the vertical one. Therefore, significant fluid flow within the two fractures takes place, thus producing energy dissipation.

Additional simulations allowed us to verify that in presence of fracture connectivity seismic attenuation is sensitive to valuable characteristics of the probed rock, namely permeabilities, lengths, intersection angles and aperture of the fractures, as well as connectivity degree of the fracture network. This indicates that a deeper understanding of this topic will reveal promising perspectives for characterization of fractured rocks.

REFERENCES

Biot, M. 1941: General theory of three-dimensional consolidation, Journal of Applied Physics, 12, 155-164.

Brajanovski, M., B. Gurevich & M. Schoenberg 2005: A model for P-wave attenuation and dispersion in a porous medium permeated by aligned fractures, Geophysical Journal International, 163, 372-384.

Rubino, J., L. Guarracino, T. Müller & K. Holliger 2013a: Do seismic waves sense fracture connectivity?, Geophysical Research Letters, 40, 692-696.

Rubino, J., L. Monachesi, T. Müller, L. Guarracino & K. Holliger 2013b: Seismic wave attenuation and dispersion due to wave-induced fluid flow in rocks with strong permeability fluctuations, Journal of the Acoustical Society of America, in press.

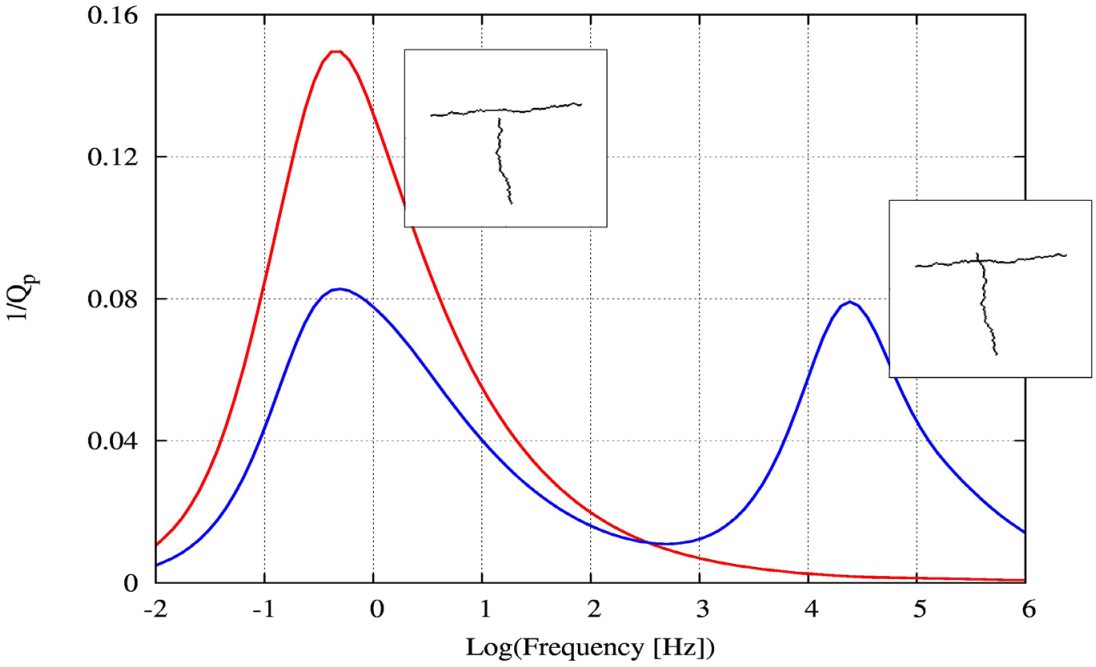

Figure 1. Inverse quality factor as a function of frequency for a rock sample containing two quasi-orthogonal fractures without (red curve) and with (blue curve) intersection.

P 11.10

Numerical modeling and laboratory measurements of seismic properties in fractured fluid reservoirs

Pei-Ju Rita Shih[1], Marcel Frehner[1]

[1]*Geological Institute, ETH Zurich, Sonneggstrasse 5, CH-8092 Zurich*
(pei-ju.shih@erdw.ethz.ch, marcel.frehner@erdw.ethz.ch)

Understanding fluid-saturated reservoir rocks is essential for the applications of, for example, CO_2 sequestration, hydrocarbon exploration, or underground nuclear waste disposal. Seismic waves are influenced by the fluids in reservoir rocks, leading to dispersion and frequency-dependent attenuation (Biot, 1962). A reliable rock characterization can be obtained if the effects of fluids filling the pore and fracture space on the seismic response are well understood.

The Krauklis wave is a unique seismic waveform, which is bound to fluid-filled fractures and propagates along fractures. It can resonate and emit seismic signals with a signature frequency. This resonant behavior should lead to a strong frequency dependence, enabling their identification in the coda (Korneev, 2008). The characteristics of Krauklis waves might be one of the keys to reveal fracture-related petrophysical parameters of reservoirs.

Several theoretical studies have demonstrated analytically the dispersion behavior of Krauklis waves in infinitely long and straight fractures (e.g., Korneev, 2008). However, purely analytical methods cannot reveal the realistic fracture geometries or finite-length fractures. Therefore, we combine numerical modeling results with laboratory experiments to visualize fracture-related effects on seismic wave propagation in reservoir rocks. Frehner and Schmalholz (2010) demonstrated that the Krauklis wave can be detected as a converted body wave as a result of scattering at the crack tip. The study also shows that the reflection behavior of the Krauklis wave depends significantly on different crack geometries and different fluids in the crack. For laboratory studies, we simulate similar conditions for a homogenous media (e.g., Plexiglas) as in the numerical experiments. We record the signatures obtained from the propagation of ultrasonic waves along samples with and without a crack, with different crack geometries and different fluids filling the crack. The design of the experiment setup thus allows us to observe and compare the effects of fluids in fractures. The comparison of numerical modeling and preliminary experimental results will be presented.

REFERENCES

Biot, M.A. 1962: Mechanics of deformation and acoustic propagation in porous media, Journal of Applied Physics, 1482-1498.

Frehner, M. & Schmalholz, S.M. 2010: Finite-element simulations of Stoneley guided-wave reflection and scattering at the tips of fluid-filled fractures, Geophysics, 75, T23-T36.

Korneev, V. 2008: Slow waves in fractures filled with viscous fluid, Geophysics, 73, N1-N7.

P 11.11

Seismic attenuation: Laboratory measurements in fluid saturated rocks

Subramaniyan Shankar[1], Madonna Claudio[1], Tisato Nicola[1], Saenger Erik[1], & Quintal Beatriz[2]

[1] *ETH Zurich, Department of Earth Sciences, Sonneggstrasse 5, CH-8092 Zurich*
(shankar.subramaniyan@erdw.ethz.ch, claudio.madonna@erdw.ethz.ch, nicola.tisato@erdw.ethz.ch, erik.saenger@erdw.ethz.ch)
[2] *University of Lausanne, Applied and Environmental Geophysics Group, Quartier UNIL-Mouline, Géopolis, CH-1015 Lausanne*
(beatriz.quintal@unil.ch)

Seismic wave attenuation could be used as an indicator of reservoir fluids due to its dependence on rock and fluid properties. Over the past 30 years, many laboratory methodologies to study attenuation in rocks have been employed, such as ultrasonic (MHz), resonant bar (kHz) and quasi-static methods in the low frequency range (0.1-100Hz) (Tisato & Madonna 2012; Madonna & Tisato 2013). Quasi-static methods have gained prominence over time as the frequency range of measurements correspond to that of field seismic data acquired for oil/gas exploration. These quasi-static experiments measure attenuation as the phase shift between the applied stress (sinusoidal) and measured strain. Since the magnitudes of measured phase shifts are quite low (Q^{-1}~0.01-0.1) and the amplitudes of strain applied to the rock samples are of the order ~10^{-6} (i.e., similar orders of magnitude to seismic waves), it is challenging. A comparison of such quasi-static setups will be presented to provide an overview of the various possibilities of design and implementation for future setups.

Several theories have been proposed in the process of identifying mechanisms causing frequency dependent attenuation in fluid saturated rocks. Wave-induced fluid flow has surfaced as the dominant mechanism and various models account for it in different ways, such as squirt flow, double porosity and patchy saturation (Pride et al. 2004). Only recently, Tisato & Quintal (2013) verified that patchy saturation can explain the frequency-dependent component of seismic attenuation measured in the laboratory for partially saturated Berea sandstone at room pressure and temperature. However, in general, there is a lack of laboratory data to test the proposed mechanisms. For example, most of the published data are for sandstones. As squirt-flow should be significant only at higher frequencies and sandstones are homogeneous in structure on the mesoscopic scale, it is relatively straightforward to attribute the observed frequency-dependent seismic attenuation to patchy saturation. Carbonates are more complicated in structure and not only patchy saturation, but also double porosity could induce significant frequency-dependent attenuation because of the heterogeneities in the solid matrix. Adam et al. (2009) observed frequency dependence in one among the five fluid saturated carbonates upon which quasi-static experiments were conducted. Currently, attenuation measurements are being carried out on samples drilled from deep carbonate reservoirs. We employ the Seismic Wave Attenuation Module (SWAM, Figure 1, Madonna & Tisato 2013) to measure seismic attenuation in these samples for different saturation degrees (90% and 100% water) and under three different confining pressures (5, 10, and 15 MPa). Preliminary results from these investigations will be discussed.

REFERENCES

Adam, L., Batzle, M., Lewallen, K. T. & van Wijk, K. 2009: Seismic wave attenuation in carbonates. Journal of Geophysical Research, doi: 10.1029/2008JB005890.

Madonna, C. & Tisato, N. 2013: A new seismic wave attenuation module to experimentally measure low-frequency attenuation in extensional mode. Geophysical Prospecting, doi: 10.1111/1365-2478.12015.

Pride, S. R., Berryman, J. G. & Harris, J. M. 2004: Seismic attenuation due to wave-induced flow. Journal of Geophysical Research, 109, B01201.

Tisato, N. & Madonna, C. 2012: Attenuation at low seismic frequencies in partially saturated rocks: Measurements and description of a new apparatus. Journal of Applied Geophysics, 86, 44-53.

Tisato, N., & Quintal, B. 2013: Measurements of seismic attenuation and transient fluid pressure in partially saturated Berea sandstone: evidence of fluid flow on the mesoscopic scale. Geophysical Journal International, doi: 10.1093/gji/ggt259.

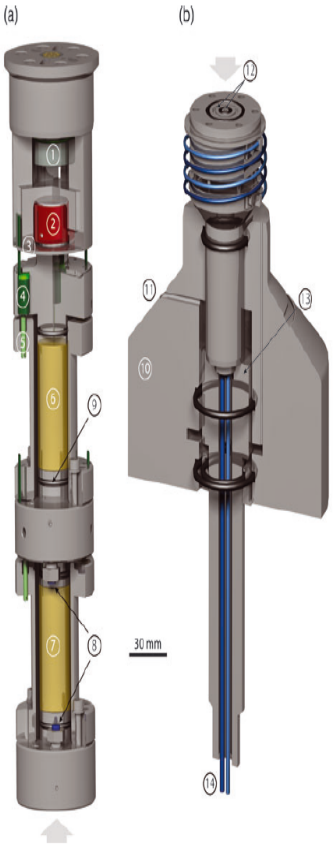

1) top plug, 2) Piezo Electric Actuator (PZA), 3) bending lamella, 4) LVDT, 5) core of the LVDT 6) reference sample (Al-Zn-Mg-Cu alloy), 7) sample 8) inlet and outlet of the pore pressure system, 9) o'ring, 10) bottom plug, 11) vent 12) inlet and outlet holes for the pore fluid, 13) pressure compensating piston, 14) inlet/outlet pipes for the pore fluid. The big grey arrows designate where part a) is connected to part b).

Figure 1. Sketch of the SWAM (after Madonna & Tisato 2013).

P 11.12

How much seismic energy is “stolen” by bubbles?

Tisato Nicola[1], Quintal Beatriz[2], and Podladchikov Yuri[2]

[1]*ETH Zurich, Zurich, Switzerland. Email: nicola.tisato@erdw.ethz.ch*
[2]*University of Lausanne, Lausanne, Switzerland.*

Wave induced fluid flow causes large attenuation and is governed by diffusion of fluids into a porous media (e.g. White, 1975). Regardless the scale at which the diffusion occurs, the fluid flow is a function of diffusivity [m^2 s^{-1}] and a pressure gradient [Pa m^{-1}]. Pressure gradient is responsible for the fluid flow. In a similar way Fick’s law can be used to model gas diffusion in liquids.

Micro bubbles (e.g. 20 µm in diameter) might be present in the pore space of rocks (Madonna et al., 2013). In an almost fully saturated porous media the strain caused by a seismic wave increases the fluid pressure and preferentially deform these bubbles. Assuming equilibrium between gas and liquid phase prior to the seismic wave propagation, variation of fluid pressure will change that. In fact, by increasing and decreasing the fluid pressure, the seismic wave will cause gas dissolution and exsolution, respectively.

Utilizing a kinetic model of gas bubble dissolution, we were able to explain attenuation measurements at tele-seismic to seismic frequencies which cannot be explained with wave induced fluid flow theories (i.e. squirt flow or patchy saturation) (Figure 1; Tisato, 2013).

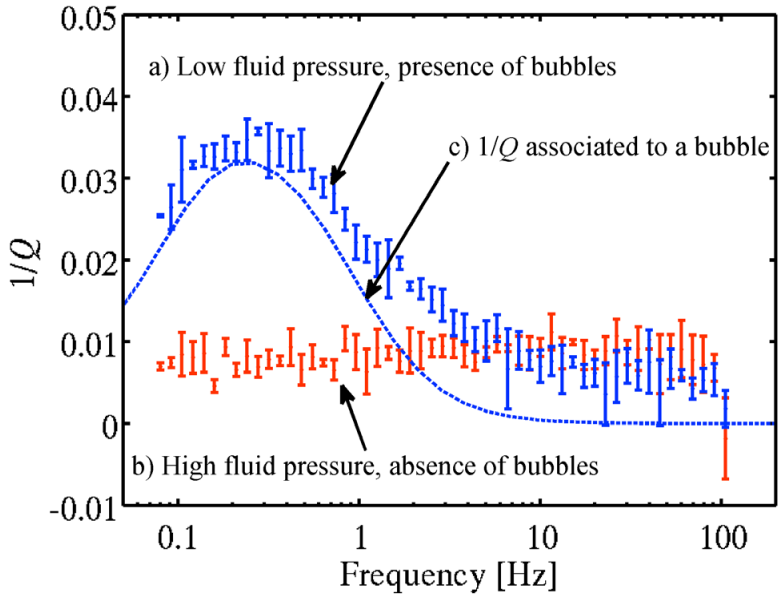

Figure 1. a) Attenuation (1/Q) for a ~100% water-glycerin saturated sample. State of stress was set to promote the formation of bubbles in the pores. b) Attenuation (1/Q) for a ~100% water-glycerin saturated sample. State of stress was set to promote the dissolution of gas in the liquid. c) Example of attenuation (1/Q) associated to a 20 mm diameter nitrogen bubble surrounded by water stressed with a sinusoidal pressure of 1 kPa.

We believe that the present contribution is of major impact for geophysics because it reports a new attenuation mechanism for partially saturated rocks operating at seismic and tele-seismic frequencies (Figure 2).

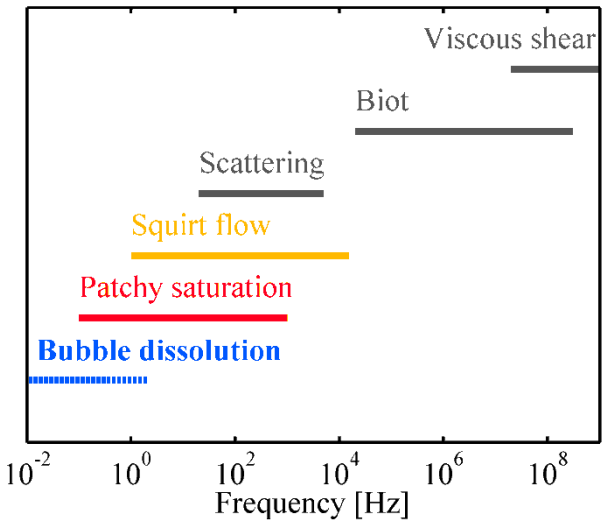

Figure 2. Attenuation mechanisms at different frequency ranges from Mavko et al. (2009) modified to include the new mechanism here proposed: Bubble Dissolution. Frequency limits for the mechanism related to Bubble Dissolution have not been yet clearly defined.

REFERENCES

Madonna, C., B. Quintal, M. Frehner, B. S. G. Almqvist, N. Tisato, M. Pistone, F. Marone, and E. H. Saenger 2013: Synchrotron-based X-ray tomographic microscopy for rock physics investigations, Geophysics, 78(1), D53–D64, doi:10.1190/geo2012-0113.1.

Mavko, G., T. Mukerji, and J. Dvorkin 2009: The rock physics handbook: tools for seismic analysis of porous media, 2nd ed., Cambridge University Press.

Tisato, N. 2013: Experimental characterization of reservoir rocks and geotechnical materials. Low frequency attenuation, ultrasonic velocities and local pore pressure effects, PhD Thesis (Diss. Nr. 21106) ETH Zurich, Switzerland.

White, J. E. 1975: Computed seismic speeds and attenuation in rocks with partial gas saturation, Geophysics, 40(2), 224–232, doi:10.1190/1.1440520.

P 11.13

Some new observations on dynamically induced fault slip

Wei Wu[1]

[1] *Ecole Polytechnique Fédérale de Lausanne (EPFL), School of Architecture, Civil and Environmental Engineering, Laboratory of Rock Mechanics (LMR), CH-1015 Lausanne (wei.wu@epfl.ch)*

A series of dynamic-induced direct-shear tests is conducted on a simulated granular fault zone. The direct-shear configuration consists of an incident norite plate (1000 × 120 × 30 mm) and a transverse norite plate (500 × 80 × 30 mm). A quartz sand layer (80 × 30 × 2 mm) is sandwiched between the incident and transverse plates to simulate a granular fault zone. A dynamic loading system containing two identical parallel compressed springs instantaneously launches a striker norite plate (100 × 120 × 30 mm) to impact the front end of the incident plate and to induce an incident P-wave (a half-wavelength of 750 mm). The P-wave propagates in the incident plate and causes the fault slip. The dynamically induced fault slip is designed to be solely induced by the P-wave before wave reflection at the plate end. It is found that the dynamic triggering induce non-uniform shear stress distribution along the fault zone. There is a shear stress at the trailing edge, which controls the fault slip, and a rebound stress at the leading edge, which is caused by a small torque (Rubinstein et al., 2004). The fault slip is triggered when the maximum shear stress reaches a critical value at the trailing edge and is accompanied by shear stress drop. By comparing with the statically induced fault slip, which is induced by a servo-controlled static loading system, it is observed that:

- The statically induced fault slip is unrecoverable and includes a main slip and a few short slips before and after the main slip, while the dynamically induced fault slip can be partially recovered after the P-wave and consists of a few unrecovered slips.
- Fault strengthening takes a long time owing to the static compaction of fault gouges (Marone, 1998). However, seismic waves successively induce fault slip and restrict fault self-healing.
- Seismic wave radiated from fault slip can reduce frictional resistance of a fault zone, which depends on local released strain energy.
- The duration of the dynamically induced fault slip is a few microseconds, while the duration of the statically induced fault slip may last from a few seconds to many years.

REFERENCES

Marone, C. 1998: The effect of loading rate on quasi-static friction and the rate of fault healing during the earthquake cycle, Nature, 391, 69-72.

Rubinstein, S.M., Cohen, C. & Fineburg, J. 2004: Detachment fronts and the onset of dynamic friction, Nature, 430, 1005-1009.

P 11.14

Effect of network density and geometric distribution on non-linear kinematic source inversion models

Youbing Zhang; Luis Dalguer; Seok Goo Song; John Clinton

Swiss Seismological Services. ETH Zurich, Switzerland

Detailed source imaging of the spatial and temporal slip distribution of earthquakes is a main research goal for seismology. In this study we investigate how the number and geometrical distribution of seismic stations affect finite kinematic source inversion results by inverting ground motions derived from a known synthetic dynamic earthquake rupture model, which is governed by the slip weakening friction law with heterogeneous stress distribution.

The target dynamic rupture model is a buried strike-slip event (Mw 6.5) in a layered half space (Dalguer & Mai, 2011) with broadband synthetic ground motions created at 168 near-field stations. A dynamic consistent regularized Yoffe function (Tinti, et al. 2005) was applied as a single window slip velocity function. And the Tikhonov regularization was used to smooth final slip. In the inversion, we modeled low frequency (under 1Hz) waveforms using a genetic algorithm in a Bayesian framework (Moneli et al. 2008) to retrieve peak slip velocity, rupture time, and rise time of the source. Three station network geometry cases were tested: (a) single station, in which we inverted 3 component waveforms from a single station varying azimuth and epicentral distance; (b) multi-station configurations with similar numbers of stations all at similar distances from, but regularly spaced around the fault; (c) irregular multi-station configurations using different numbers of stations. For analysis, waveform misfits are calculated using all 168 stations.

Our preliminary results show: 1) single station tests suggest that it may be possible to obtain a relatively good source model even using one station, with a waveform misfit comparable to that obtained with the best source model. The best single station performance occurs with stations in which amplitude ratios between the three components are not large, indicating that P and S waves are all present. We infer that both body wave radiation pattern and distance play an important role in the selection of optimal station. 2) Multi-station tests indicate irregular distribution of stations with different azimuths and distances around the fault provides the best source models. The minimum waveform misfit is obtained using the all-168 stations, but source model is not significant improved by using denser network. It suggests the best source model is not necessarily derived from the model with minimum waveform misfit. 3) Number of stations affects the estimated source image, but a surprisingly small number of well-spaced stations appear sufficient to obtain acceptable solutions in our study.